Journal of General Virology (2009), **90**, 2849–2854 DOI 10.1099/vir.0.014514-0

Short Communication

Phylogeny and primary structure analysis of fiber shafts of all human adenovirus types for rational design of adenoviral gene-therapy vectors

Sebastian Darr, Ijad Madisch, Sören Hofmayer, Fabienne Rehren and Albert Heim

Institut für Virologie, Medizinische Hochschule Hannover, D-30625 Hannover, Germany

Correspondence
Albert Heim
Heim.Albert@mh-hannover.de

Received 19 June 2009
Accepted 4 August 2009

The fiber shaft of human adenoviruses (HAdVs) is essential for bringing the penton base into proximity to the secondary cellular receptor. Fiber shaft sequences of all 53 HAdV types were studied. Phylogeny of the fiber shaft revealed clustering corresponding to the HAdV species concept. An intraspecies recombination hot spot was found at the shaft/knob boundary, a highly conserved sequence stretch. For example, HAdV-D20 clustered with HAdV-D23 in the fiber shaft, but with HAdV-D47 in the fiber knob. Although all shafts exhibited the typical pseudorepeats, amino acid sequence identity was found to be as high as 92 % (interspecies) and 54 % (intraspecies). In contrast to a previous study, a flexibility motif (KXGGLXFD/N) was found in eight HAdV-D types, whereas the putative heparan sulfate-binding site (KKTK) was only found in species HAdV-C. Our results suggest that pseudotyping of gene-therapy vectors at the shaft/knob boundary is feasible, but that flexibility data of shafts should be considered.

Members of the family *Adenoviridae* are double-stranded DNA viruses with a non-enveloped, icosahedral capsid (Swenson *et al.*, 2003). The 53 human adenovirus (HAdV) types are grouped into six recognized species (HAdV-A to -F) and a proposed seventh species (HAdV-G), which were defined historically on the basis of haemagglutination properties, oncogenic properties in rodents and DNA homology. The viruses are mainly responsible for causing respiratory-tract illness (HAdV-B3, -B7, -B21, -E4, -C1, -C2 and -C5), gastroenteric infections (HAdV-A12, -A18, -A31, -F40 and -F41) and ocular infections (HAdV-D8, -D19 and -D37).

Adenovirus capsids consist in total of 240 copies of trimeric hexon protein, and a penton complex at each of the 12 vertices. The penton is made of a pentameric base and a trimeric fiber. The fiber is organized in three well-defined regions that play an important role in adenovirus infectivity (Shenk, 2001). These are the amino-terminal 'tail' that binds to the penton base, a central 'shaft' of variable length and a carboxy-terminal 'knob' domain. The HAdV-C2 fiber shaft was the first to be analysed in detail by Green *et al.* (1983), who suggested pseudorepeats of 15 residues consisting of two short β-strands and two β-bends. The fiber knob interacts with primary cellular receptors, e.g. coxsackievirus–adenovirus receptor (CAR), CD46, CD86 and sialic acid (Marttila *et al.*, 2005; Roelvink *et al.*, 1998; Seiradake *et al.*, 2009; Short *et al.*, 2004; Sirena *et al.*, 2004). Primary binding to cells is followed by cell entry after interaction of the RGD tripeptide loop extending from the penton base with cellular $\alpha_v\beta_3$ or $\alpha_v\beta_5$ integrins (Bai *et al.*, 1994; Mathias *et al.*, 1994; Schoehn *et al.*, 1996; Wickham *et al.*, 1993). The flexibility of the fiber shaft seems to be essential to bring the penton base into close proximity to the secondary receptor after the primary receptor interaction. Two flexibility loops have been described in the fiber shaft of most HAdV types, but they have not been found in species HAdV-D (Chroboczek *et al.*, 1995). Furthermore, a putative heparan sulfate-binding site [KKTK or, in general, BBXB and BBBXXB, where 'B' stands for a basic amino acid such as Lys, Arg or His (Templeton, 1992)] was found in the fiber shafts of species HAdV-C serotypes, but not in other HAdV species.

The virus enters host cells by a process termed receptor-mediated endocytosis (Maxfield & McGraw, 2004) via clathrin-coated pits using dynamin-mediated endocytosis (Li *et al.*, 1998; Morgan *et al.*, 1969; Nemerow & Stewart, 1999; Wang *et al.*, 1998). Cell entry is followed by an interaction with cytosolic molecular motors, which drive the capsid along microtubules (Mabit *et al.*, 2002; Suomalainen *et al.*, 2001) through the microtubule-organizing centre to the nucleus (Kelkar *et al.*, 2004).

Even though the adenovirus fiber shaft is essential for infectivity and understanding of virus tropism (Nakamura *et al.*, 2003; Roelvink *et al.*, 1998; Seki *et al.*, 2002;

The GenBank/EMBL/DDBJ accession numbers for newly generated sequences are FM210540–FM210562 and FN397565–FN397571.

Supplementary figures and tables are available with the online version of this paper.

Shayakhmetov & Lieber, 2000; Smith *et al.*, 2003; Vigne *et al.*, 2003), a complete dataset of fiber shaft sequences has not been available to date. In this study, fiber shaft sequences were generated and a complete dataset of all 53 HAdV types and eight simian adenovirus (SAdV) types, which belong to the HAdV species, was used to study the primary structure of the fiber shaft and to predict flexibility loops and heparan sulfate-binding sites. Furthermore, clustering of the fiber shaft region was compared with that of the fiber knob in order to search for recombination events in the evolution of HAdV types.

HAdV prototype strains were obtained from the ATCC, except for HAdV-B14, -D10, -D13 and -D30 prototype strains, which were obtained from our collection at the German National Reference Laboratory for Adenoviruses, Hannover Medical School, Germany. DNA was extracted with a Qiagen blood kit. Fiber shaft amplicons for species HAdV-D were generated by PCR using primers displayed in Supplementary Table S1 (available in JGV Online). PCR products were separated in 2 % agarose gel and extracted from the gel with a Qiagen gel extraction kit. Cycle sequencing was performed with PCR primers and rhodamine-labelled dideoxynucleotide chain terminators (ABI) and an ABI Prism 310 or ABI 3130 automatic sequencer. The generated fiber shaft sequences were deposited in GenBank under accession numbers FM210540–FM210562 (see Supplementary Table S2, available in JGV Online). Multiple alignments were generated by sequential pairwise alignment using the CLUSTAL algorithm implemented in the BioEdit software package (version 6.0.5; Hall, 1999) and adjusted manually to conform to the optimized alignment of deduced amino acid sequences. Phylogenetic trees of the fiber shaft region based on nucleotide positions 31162–32239 (referring to the HAdV-C2 fiber shaft sequence; GenBank accession no. J01917) were constructed with the help of MEGA software (version 4; Tamura *et al.*, 2007) with several phylogenetic-reconstruction algorithms (neighbour joining, minimum evolution and maximum parsimony) and were congruent in overall structure (Fig. 1 depicts neighbour-joining trees).

Sequences of adenovirus fiber shaft clustered according to the species concept, as observed previously for the hexon ε determinant, the penton base δ determinant and the γ determinant of the fiber knob (Madisch *et al.*, 2005, 2007). Clustering was supported by high bootstrap values. Interspecies variability in the shaft region was higher (55–93 % amino acid sequence divergence) than in the fiber knob region (50–59 %) (Madisch *et al.*, 2007); in contrast, intraspecies divergence was higher in the knob region (18–53 % amino acid sequence divergence) than in the fiber shaft (18–44 %). Surprisingly, all HAdV species except for HAdV-B showed a lower intraspecies ratio of synonymous/non-synonymous (S/N) mutations in the fiber shaft (e.g. HAdV-D, 2.2) than in the fiber knob (e.g. HAdV-D, 3.03). This suggests that more positive selection occurs in the fiber shaft region, although the fiber knob contains a well-established immunogenic determinant (γ).

Both the tail/shaft boundary and the shaft/knob boundary were highly conserved throughout all adenovirus subtypes, with a completely conserved GVL sequence and a conserved TLWT motif, respectively. However, species HAdV-F has two fibers of different lengths expressed at a relative ratio of 1 : 1 (Albinsson & Kidd, 1999; Favier *et al.*, 2002; Kidd *et al.*, 1990, 1993; Yeh *et al.*, 1994) (Supplementary Fig. S1, available in JGV Online). Surprisingly, the short fibers have a TIWS sequence as the fiber shaft/knob boundary and an amino acid sequence identity of only 41 % to the long shafts, suggesting that one of the fibers was acquired from another HAdV species (Kidd *et al.*, 1993) (Fig. 1a). As only the long fiber is able to interact with CAR (Roelvink *et al.*, 1998), the short one may bind to an additional, as-yet-unknown receptor mainly expressed in the gastrointestinal tract (Favier *et al.*, 2002), explaining the tropism of HAdV-F.

Comparison of phylogenetic trees of fiber shaft and knob suggested several intraspecies-recombination events in the phylogeny of 10 (of 33) HAdV-D prototypes, because of different clustering confirmed by high bootstrap values (Fig. 1). For example, HAdV-D20 clustered with HAdV-D23 in the fiber shaft region, whereas it clustered with HAdV-D47 in the fiber knob region. Bootscans were performed with the software SimPlot (version 3.5.1; Lole *et al.*, 1999) with a window of 200 bp (20 bp step) based on a Kimura two-parameter substitution model (Kimura, 1980) with a transition/transversion ratio of 2.0 (Fig. 2). Bootscan results determined a recombination hot spot at the shaft/knob boundary [nucleotide position 440, referring to HAdV-D20 (GenBank accession no. AJ811444) in a complete fiber alignment], a highly conserved region that is prone to promoting homologous recombination (Supplementary Fig. S2, available in JGV Online). These recombination events in species HAdV-D, with several prototypes sharing identical shaft sequences, suggested the feasibility of a fiber knob-replacement strategy for pseudotyping of gene-therapy vectors with a species HAdV-D-derived fiber gene. As the fiber knob contains the major receptor-binding site, fiber knob pseudotyping holds promise to modify tropism. Species HAdV-D-derived gene-therapy vectors were developed recently for the treatment of malignant melanoma and soft-tissue sarcoma (Hoffmann *et al.*, 2007, 2008).

Furthermore, we included seven intermediate HAdV-D strains (HAdV-D15H9, -D17H29, -D19H30, -D30H44, -D37H13, -D37H17 and -D46H13) in our phylogenetic analysis. Previously, these strains had been typed with contradictory results by neutralization testing (hexon ε determinant) and haemagglutination-inhibition testing (γ determinant of fiber knob), indicating at least one recombination event between the hexon gene and the fiber knob-encoding region. However, a detailed genetic analysis of these intermediate strains had not yet been performed. Only one of seven HAdV-D intermediate strains (HAdV-D19H30) was recombinant at the fiber shaft/knob boundary hot spot (Supplementary Fig. S3, available in JGV Online). Surprisingly, the fiber shaft of HAdV-

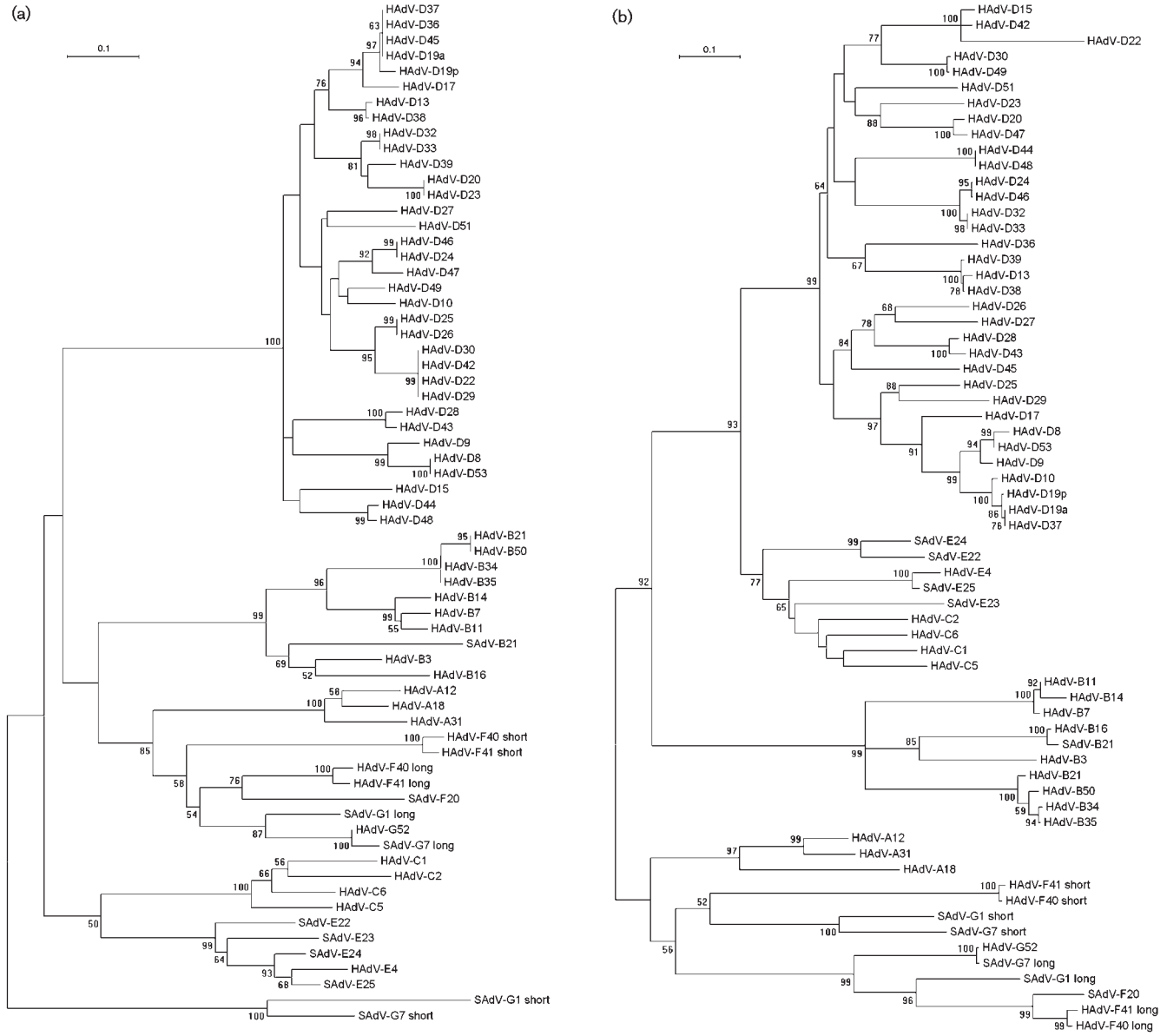

Fig. 1. Phylogenetic trees (neighbour joining) of the nucleic acid sequences of (a) the fiber shaft domain (1077 bp, referring to HAdV-C1; GenBank accession no. AC000017) and (b) the fiber knob domain (522 bp, referring to HAdV-C1). Bootstrap values (%) were generated with 1000 pseudoreplicates. In addition to the newly generated fiber shaft sequences, reference sequences from GenBank were used; see Supplementary Table S2 (available in JGV Online) for details.

D19H30 was related closely to that of HAdV-D49, whereas it clustered immediately adjacent to HAdV-D30 in the fiber knob region, supported by high bootstrap values (Supplementary Fig. S4, available in JGV Online). This result indicated another recombination event in the genome of HAdV-D19H30 between the hexon gene and the fiber gene, suggesting a multiple-recombinant HAdV isolate similar to the recently published novel HAdV type D53 (Walsh *et al.*, 2009). Recently, frequent recombination events were also described in the phylogeny of species HAdV-C field isolates (Lukashev *et al.*, 2008).

A complete overview of the length of all human adenovirus fiber shafts was generated (Supplementary Fig. S1). All fiber shaft sequences were congruent to the cross-β model of pseudorepeats, which contains two β-strands and two turns (Green *et al.*, 1983). The highest number of pseudorepeats was found in species HAdV-A (23) and the lowest in species HAdV-B (six). Several HAdV types revealed differences in the length of their fiber shafts in comparison to other HAdV types of their species, e.g. HAdV-B16 (30 aa, about two pseudorepeats longer), HAdV-A31 (31 aa, about two pseudorepeats shorter) and

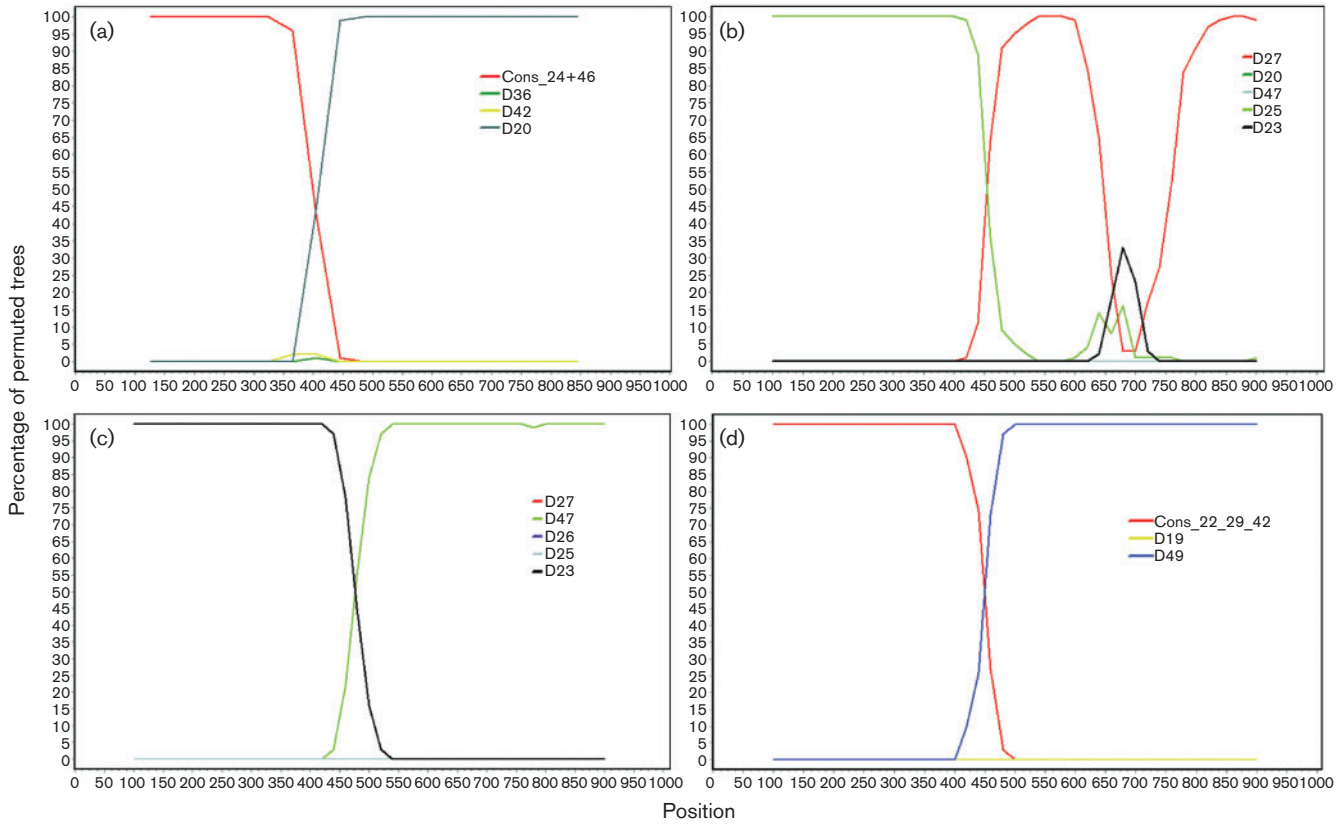

Fig. 2. Bootscan analysis performed with SimPlot revealed recombination events at the shaft/knob boundary in the phylogeny of HAdV-D types HAdV-D47 (a), -D26 (b), -D20 (c) and -D30 (d).

HAdV-C6 (51 aa, about three pseudorepeats shorter). These differences in length may also influence flexibility of the fiber shaft.

All HAdV-D shafts consisted of eight pseudorepeats with a length between 140 and 148 aa. HAdVs of species D can be divided into three groups according to the length of their fiber shaft. The first group, with fiber shaft lengths between 140 and 142 aa, consisted of types HAdV-D8, -D9, -D15, -D28, -D43, -D44 and -D48; the second, with a length of 145 aa, consisted of types HAdV-D17, -D19, -D37, -D36 and -D45, and the third group, with a length of 147 or 148 aa, consisted of all remaining HAdV-D types.

The entire fiber shaft dataset finally allows determination of the absence of a heparan sulfate-binding site (KKTK motif) in all HAdVs other than species HAdV-C. This included a search for any general motif, BBXB or BBBXXB (where 'B' stands for a basic amino acid such as Lys, Arg or His).

The heparan sulfate-binding site was formerly described as a sufficient receptor for initial binding of several HAdVs

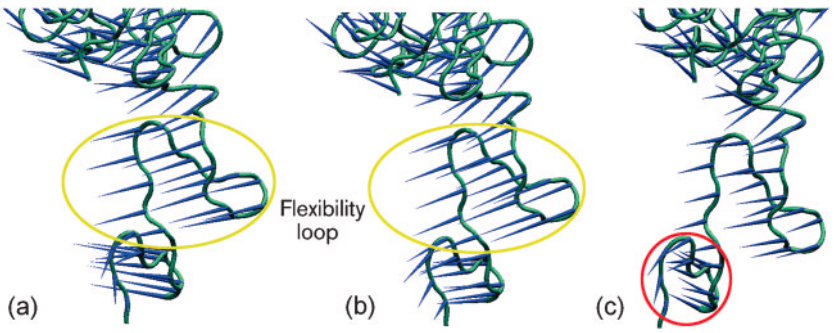

Fig. 3. Porcupine molecular-dynamic representation of the fiber shaft/knob boundary including the second flexibility loop of HAdV-C2 (a), which was also predicted for HAdV-D23 (b). For comparison, HAdV-D17 (c) is depicted, which also had differences in the adjacent amino-terminal loop (red circle).

(Dechecchi *et al.*, 2001). In contrast, recent studies demonstrated that the KKTK motif of the fiber shaft plays only a minimal role, if any, in the binding of heparan sulfate glycosaminoglycans, but is important for post-internalization steps of virus infection, especially trafficking to the nucleus (Kritz *et al.*, 2007).

Adenovirus fiber shafts of all HAdVs except species HAdV-D contain a different number of residues in the third pseudorepeat that are thought to allow bending of the fiber shaft (Chroboczek *et al.*, 1995; Wu *et al.*, 2003). Our complete sequence dataset of fiber shaft sequences now demonstrates the absence of this flexibility loop in any of the 33 species D adenoviruses.

A second flexibility loop (the KLGXGLXFD/N sequence, where X stands for any amino acid) is located in the penultimate pseudorepeat of the fiber shaft. After analysing the fiber shaft sequences of HAdV-D8, -D9 and -D15, it was assumed that all HAdV-D adenoviruses lack this second flexibility loop, in contrast to all other HAdV species (Chroboczek *et al.*, 1995). However, our complete dataset of adenovirus fiber shaft sequences demonstrated a KDGGLXFD/N motif in eight HAdV-D prototypes (HAdV-D20, -D23, -D24, -D32, -D33, -D46, -D47 and -D51), which is only 1 aa shorter than the formerly described motif.

The flexibility of the proposed KDGGLXFD/N motif in HAdV-D23 was analysed *in silico* in comparison to HAdV-D17 (without a flexibility loop) and HAdV-C2 (with the flexibility-loop sequence KLGXGLXFD/N). For this purpose, homology models of the partial fiber protein were initially produced and visualized by using the Swiss-PdbViewer protein-modelling environment (version 4.01; Guex & Peitsch, 1997) and VMD (version 1.8.6; Humphrey *et al.*, 1996). Based on the crystallography fiber data of HAdV-C2 (Pdb accession no. 1QIU), predictions for HAdV-D23 and -D17 were performed by using a structural alignment to guide the threading of model sequences onto the known molecular structures using the Swiss-PdbViewer software. A CONCOORD-based simulation and principal-component analysis on the resulting ensemble was performed with the Dynamite web server (Barrett *et al.*, 2004). A higher flexibility was displayed by the length of the dark-blue spikes of both HAdV-D23 and HAdV-C2 compared with HAdV-D17 in porcupine molecular-dynamic diagrams of the fiber shaft/knob boundary (Fig. 3). This suggested that the proposed flexibility motif KDGGLXFD/N of species HAdV-D is functional. This may also imply higher infectivity, as previous studies suggested that the flexibility of adenovirus fiber shafts was crucial for adenovirus–receptor interaction (Wu *et al.*, 2003).

In conclusion, positive selection of fiber shaft mutations as strong as seen in the fiber knob region was indicated by the high intra- and interspecies divergence and low S/N values. Moreover, a recombination hot spot was found at the shaft/knob boundary of species HAdV-D and may be used in future for efficient pseudotyping in the design of HAdV-D gene-therapy vectors. Further work is needed to determine whether differences in HAdV-D fiber structure influence organ tropism.

Acknowledgements

We would like to thank Mark van Raaij (Instituto de Biologia Molecular de Barcelona, Barcelona, Spain) for his help in modelling the HAdV-C2 fiber X-ray diffraction file and Kelly Te for critical reading of the manuscript.

References

Albinsson, B. & Kidd, A. H. (1999). Adenovirus type 41 lacks an RGD α_v-integrin binding motif on the penton base and undergoes delayed uptake in A549 cells. *Virus Res* **64**, 125–136.

Bai, M., Campisi, L. & Freimuth, P. (1994). Vitronectin receptor antibodies inhibit infection of HeLa and A549 cells by adenovirus type 12 but not by adenovirus type 2. *J Virol* **68**, 5925–5932.

Barrett, C. P., Hall, B. A. & Noble, M. E. (2004). Dynamite: a simple way to gain insight into protein motions. *Acta Crystallogr D Biol Crystallogr* **60**, 2280–2287.

Chroboczek, J., Ruigrok, R. W. & Cusack, S. (1995). Adenovirus fiber. *Curr Top Microbiol Immunol* **199**, 163–200.

Dechecchi, M. C., Melotti, P., Bonizzato, A., Santacatterina, M., Chilosi, M. & Cabrini, G. (2001). Heparan sulfate glycosaminoglycans are receptors sufficient to mediate the initial binding of adenovirus types 2 and 5. *J Virol* **75**, 8772–8780.

Favier, A. L., Schoehn, G., Jaquinod, M., Harsi, C. & Chroboczek, J. (2002). Structural studies of human enteric adenovirus type 41. *Virology* **293**, 75–85.

Green, N. M., Wrigley, N. G., Russell, W. C., Martin, S. R. & McLachlan, A. D. (1983). Evidence for a repeating cross-beta sheet structure in the adenovirus fibre. *EMBO J* **2**, 1357–1365.

Guex, N. & Peitsch, M. C. (1997). SWISS-MODEL and the Swiss-PdbViewer: an environment for comparative protein modeling. *Electrophoresis* **18**, 2714–2723.

Hall, T. A. (1999). BioEdit: a user-friendly biological sequence alignment editor and analysis program for Windows 95/98/NT. *Nucleic Acids Symp Ser* **41**, 95–98.

Hoffmann, D., Heim, A., Nettelbeck, D. M., Steinstraesser, L. & Wildner, O. (2007). Evaluation of twenty human adenoviral types and one infectivity-enhanced adenovirus for the therapy of soft tissue sarcoma. *Hum Gene Ther* **18**, 51–62.

Hoffmann, D., Bayer, W., Heim, A., Potthoff, A., Nettelbeck, D. M. & Wildner, O. (2008). Evaluation of twenty-one human adenovirus types and one infectivity-enhanced adenovirus for the treatment of malignant melanoma. *J Invest Dermatol* **128**, 988–998.

Humphrey, W., Dalke, A. & Schulten, K. (1996). VMD: visual molecular dynamics. *J Mol Graph* **14**, 33–38.

Kelkar, S. A., Pfister, K. K., Crystal, R. G. & Leopold, P. L. (2004). Cytoplasmic dynein mediates adenovirus binding to microtubules. *J Virol* **78**, 10122–10132.

Kidd, A. H., Erasmus, M. J. & Tiemessen, C. T. (1990). Fiber sequence heterogeneity in subgroup F adenoviruses. *Virology* **179**, 139–150.

Kidd, A. H., Chroboczek, J., Cusack, S. & Ruigrok, R. W. (1993). Adenovirus type 40 virions contain two distinct fibers. *Virology* **192**, 73–84.

Kimura, M. (1980). A simple method for estimating evolutionary rates of base substitutions through comparative studies of nucleotide sequences. *J Mol Evol* **16**, 111–120.

Kritz, A. B., Nicol, C. G., Dishart, K. L., Nelson, R., Holbeck, S., Von Seggern, D. J., Work, L. M., McVey, J. H., Nicklin, S. A. & Baker, A. H. (2007). Adenovirus 5 fibers mutated at the putative HSPG-binding site show restricted retargeting with targeting peptides in the HI loop. *Mol Ther* **15**, 741–749.

Li, E., Stupack, D., Bokoch, G. M. & Nemerow, G. R. (1998). Adenovirus endocytosis requires actin cytoskeleton reorganization mediated by Rho family GTPases. *J Virol* **72**, 8806–8812.

Lole, K. S., Bollinger, R. C., Paranjape, R. S., Gadkari, D., Kulkarni, S. S., Novak, N. G., Ingersoll, R., Sheppard, H. W. & Ray, S. C. (1999). Full-length human immunodeficiency virus type 1 genomes from subtype C-infected seroconverters in India, with evidence of intersubtype recombination. *J Virol* **73**, 152–160.

Lukashev, A. N., Ivanova, O. E., Eremeeva, T. P. & Iggo, R. D. (2008). Evidence of frequent recombination among human adenoviruses. *J Gen Virol* **89**, 380–388.

Mabit, H., Nakano, M. Y., Prank, U., Saam, B., Dohner, K., Sodeik, B. & Greber, U. F. (2002). Intact microtubules support adenovirus and herpes simplex virus infections. *J Virol* **76**, 9962–9971.

Madisch, I., Harste, G., Pommer, H. & Heim, A. (2005). Phylogenetic analysis of the main neutralization and hemagglutination determinants of all human adenovirus prototypes as a basis for molecular classification and taxonomy. *J Virol* **79**, 15265–15276.

Madisch, I., Hofmayer, S., Moritz, C., Grintzalis, A., Hainmueller, J., Pring-Akerblom, P. & Heim, A. (2007). Phylogenetic analysis and structural predictions of human adenovirus penton proteins as a basis for tissue-specific adenovirus vector design. *J Virol* **81**, 8270–8281.

Marttila, M., Persson, D., Gustafsson, D., Liszewski, M. K., Atkinson, J. P., Wadell, G. & Arnberg, N. (2005). CD46 is a cellular receptor for all species B adenoviruses except types 3 and 7. *J Virol* **79**, 14429–14436.

Mathias, P., Wickham, T., Moore, M. & Nemerow, G. (1994). Multiple adenovirus serotypes use αv integrins for infection. *J Virol* **68**, 6811–6814.

Maxfield, F. R. & McGraw, T. E. (2004). Endocytic recycling. *Nat Rev Mol Cell Biol* **5**, 121–132.

Morgan, C., Rosenkranz, H. S. & Mednis, B. (1969). Structure and development of viruses as observed in the electron microscope. V. Entry and uncoating of adenovirus. *J Virol* **4**, 777–796.

Nakamura, T., Sato, K. & Hamada, H. (2003). Reduction of natural adenovirus tropism to the liver by both ablation of fiber–coxsackievirus and adenovirus receptor interaction and use of replaceable short fiber. *J Virol* **77**, 2512–2521.

Nemerow, G. R. & Stewart, P. L. (1999). Role of α_v integrins in adenovirus cell entry and gene delivery. *Microbiol Mol Biol Rev* **63**, 725–734.

Roelvink, P. W., Lizonova, A., Lee, J. G., Li, Y., Bergelson, J. M., Finberg, R. W., Brough, D. E., Kovesdi, I. & Wickham, T. J. (1998). The coxsackievirus–adenovirus receptor protein can function as a cellular attachment protein for adenovirus serotypes from subgroups A, C, D, E, and F. *J Virol* **72**, 7909–7915.

Schoehn, G., Fender, P., Chroboczek, J. & Hewat, E. A. (1996). Adenovirus 3 penton dodecahedron exhibits structural changes of the base on fibre binding. *EMBO J* **15**, 6841–6846.

Seiradake, E., Henaff, D., Wodrich, H., Billet, O., Perreau, M., Hippert, C., Mennechet, F., Schoehn, G., Lortat-Jacob, H. & other authors (2009). The cell adhesion molecule "CAR" and sialic acid on human erythrocytes influence adenovirus *in vivo* biodistribution. *PLoS Pathog* **5**, e1000277.

Seki, T., Dmitriev, I., Kashentseva, E., Takayama, K., Rots, M., Suzuki, K. & Curiel, D. T. (2002). Artificial extension of the adenovirus fiber shaft inhibits infectivity in coxsackievirus and adenovirus receptor-positive cell lines. *J Virol* **76**, 1100–1108.

Shayakhmetov, D. M. & Lieber, A. (2000). Dependence of adenovirus infectivity on length of the fiber shaft domain. *J Virol* **74**, 10274–10286.

Shenk, T. (2001). *Adenoviridae*: the viruses and their replication. In *Fields Virology*, 4th edn, pp. 2265–2299. Edited by D. M. Knipe, M. Howley, D. E. Griffin, R. A. Lamb, M. A. Matin, B. Roizman & S. E. Straus. Philadelphia, PA: Lippincott Williams & Wilkins.

Short, J. J., Pereboev, A. V., Kawakami, Y., Vasu, C., Holterman, M. J. & Curiel, D. T. (2004). Adenovirus serotype 3 utilizes CD80 (B7.1) and CD86 (B7.2) as cellular attachment receptors. *Virology* **322**, 349–359.

Sirena, D., Lilienfeld, B., Eisenhut, M., Kalin, S., Boucke, K., Beerli, R. R., Vogt, L., Ruedl, C., Bachmann, M. F. & other authors (2004). The human membrane cofactor CD46 is a receptor for species B adenovirus serotype 3. *J Virol* **78**, 4454–4462.

Smith, T. A., Idamakanti, N., Rollence, M. L., Marshall-Neff, J., Kim, J., Mulgrew, K., Nemerow, G. R., Kaleko, M. & Stevenson, S. C. (2003). Adenovirus serotype 5 fiber shaft influences *in vivo* gene transfer in mice. *Hum Gene Ther* **14**, 777–787.

Suomalainen, M., Nakano, M. Y., Boucke, K., Keller, S. & Greber, U. F. (2001). Adenovirus-activated PKA and p38/MAPK pathways boost microtubule-mediated nuclear targeting of virus. *EMBO J* **20**, 1310–1319.

Swenson, P. D., Wadell, G., Allard, A. & Hierholzer, J. C. (2003). Adenoviruses. In *Manual of Clinical Microbiology*. Edited by P. R. Murray, E. J. Baron, M. A. Pfaller, J. H. Jorgensen & R. A. Yolken. Washington, DC: American Society for Microbiology.

Tamura, K., Dudley, J., Nei, M. & Kumar, S. (2007). MEGA4: molecular evolutionary genetics analysis (MEGA) software version 4.0. *Mol Biol Evol* **24**, 1596–1599.

Templeton, D. M. (1992). Proteoglycans in cell regulation. *Crit Rev Clin Lab Sci* **29**, 141–184.

Vigne, E., Dedieu, J. F., Brie, A., Gillardeaux, A., Briot, D., Benihoud, K., Latta-Mahieu, M., Saulnier, P., Perricaudet, M. & Yeh, P. (2003). Genetic manipulations of adenovirus type 5 fiber resulting in liver tropism attenuation. *Gene Ther* **10**, 153–162.

Walsh, M. P., Chintakuntlawar, A., Robinson, C. M., Madisch, I., Harrach, B., Hudson, N. R., Schnurr, D., Heim, A., Chodosh, J. & other authors (2009). Evidence of molecular evolution driven by recombination events influencing tropism in a novel human adenovirus that causes epidemic keratoconjunctivitis. *PLoS One* **4**, e5635.

Wang, K., Huang, S., Kapoor-Munshi, A. & Nemerow, G. (1998). Adenovirus internalization and infection require dynamin. *J Virol* **72**, 3455–3458.

Wickham, T. J., Mathias, P., Cheresh, D. A. & Nemerow, G. R. (1993). Integrins $\alpha_v\beta_3$ and $\alpha_v\beta_5$ promote adenovirus internalization but not virus attachment. *Cell* **73**, 309–319.

Wu, E., Pache, L., Von Seggern, D. J., Mullen, T. M., Mikyas, Y., Stewart, P. L. & Nemerow, G. R. (2003). Flexibility of the adenovirus fiber is required for efficient receptor interaction. *J Virol* **77**, 7225–7235.

Yeh, H. Y., Pieniazek, N., Pieniazek, D., Gelderblom, H. & Luftig, R. B. (1994). Human adenovirus type 41 contains two fibers. *Virus Res* **33**, 179–198.